

THE CRYSTAL STRUCTURES OF COSTIBITE (CoSbS) AND PARACOSTIBITE (CoSbS)*

J. F. ROWLAND, E. J. GABE**, AND S. R. HALL
*Mineral Sciences Division, Mines Branch, Department of Energy,
Mines and Resources, 555 Booth Street, Ottawa, Canada*

ABSTRACT

The crystal structures of natural costibite and synthetic paracostibite, two forms of CoSbS, have been refined by three-dimensional x-ray diffraction techniques to R-values of 0.046 and 0.053, respectively. Costibite is orthorhombic, with $a = 4.873(2)$, $b = 5.852(3)$, $c = 3.608(1)\text{\AA}$, $Z = 2$, and space group $Pn2_1m$. Paracostibite is orthorhombic, with $a = 5.842(3)$, $b = 5.951(3)$, $c = 11.666(4)\text{\AA}$, $Z = 8$, and space group $Pbca$. The structures are similar to those of rammelsbergite and parammelsbergite, respectively, and the paracostibite structure can be described as consisting of portions of the costibite structure combined in two orientations.

INTRODUCTION

Until recently no minerals of the composition CoSbS were known, with the possible exception of the hypothetical end-member of the willyamite series, which has the composition (Co,Ni)SbS with $\text{Co} > \text{Ni}$ (Cabri *et al.* 1970). Two minerals, costibite and paracostibite, have been found in samples from Broken Hill, N.S.W., Australia, and Red Lake, Ontario, Canada, re-

spectively, by Cabri, Harris & Stewart (1970a, 1970b). The microprobe analysis reported for costibite is included in Table 1. The name of costibite was given because of its composition, and that of paracostibite because of its analogous relationship to the rammelsbergite-parammelsbergite series. Attempts to synthesize CoSbS at these laboratories have always resulted in a structure corresponding to paracostibite. The powder diffraction pattern is essentially the same as that for natural material.

EXPERIMENTAL

Suitable crystals of natural costibite from Broken Hill were available, but the paracostibite crystals from Red Lake were too fine-grained, and crystals of synthetic material were used. A preliminary survey using precession camera techniques confirmed that the orthorhombic cells used to index the powder diffraction patterns were correct.

The crystal fragments of both materials were irregular in shape and approximately 0.05 mm in dimension. The orientation matrices were determined and the cell dimensions were calculated on a Picker 4-circle diffractometer using an automatic alignment process (Busing 1970). For costibite the 2θ , χ and ω angles were obtained from 42 reflections, with 2θ between 64° and 70° , consisting of the equivalents of 623,

*Mineral Research Program: Sulphide Research Contribution No. 89.

**Present address: Chemistry Division, National Research Council of Canada, Ottawa, Canada.

TABLE 1. CRYSTAL DATA

	Costibite	Paracostibite		Costibite	Paracostibite
Source	Consols Lode, Broken Hill, N.S.W., Australia (Smithsonian Institution, Washington, D.C., U.S.A. National Museum No. R849)	Synthesized in Mineralogy Section, Mineral Sciences Division, Mines Branch, Ottawa, Ontario, Canada	Space Group	$Pn2_1m$ (No. 31)	$Pbca$ (No. 61)
			Cell Dimensions	$a = 4.873(2)$ $b = 5.852(3)$ $c = 3.608(1)\text{\AA}$	$a = 5.842(3)$ $b = 5.951(3)$ $c = 11.666(4)\text{\AA}$
Microprobe Analysis (wt %)	(averages for 3 grains) Co 26.7 ± 0.5 Fe 0.6 ± 0.05 Ni 0.2 ± 0.05 Sb 57.0 ± 0.5 As 0.3 ± 0.1 S 13.1 ± 0.5 Total = 99.9%	(starting composition, one phase only detected by microscopic and microprobe analysis) Co 27.70 Sb 57.23 S 15.07 Total = 100.00%	Cell Content	$\text{Co}_2\text{Sb}_2\text{S}_2$ (Z=2)	$\text{Co}_8\text{Sb}_8\text{S}_8$ (Z=8)
			Density	6.9 g/cm ³ (meas.) 6.87 g/cm ³ (calc.)	6.9 g/cm ³ (meas.) 6.97 g/cm ³ (calc.)
			Absorption	$\mu = 220\text{ cm}^{-1}$	$\mu = 220\text{ cm}^{-1}$
			Reflections	894 (measured 3 times)	3085 (measured 1 time)
Chemical Composition	$(\text{Co}_{2.95}\text{Fe}_{0.02}\text{Ni}_{0.01})(\text{Sb}_{1.00}\text{As}_{0.01})\text{S}_{1.00}$	$\text{Co}_{1.00}\text{Sb}_{1.00}\text{S}_{1.00}$	Significant Intensities	843 (>10% level)	1886 (>10% level)
System	Orthorhombic	Orthorhombic			

TABLE 2. STRUCTURE DATA

	Atom	Site	Atomic Coordinates			Temperature Factors* (x 100)					
			x	y	z	U ₁₁	U ₂₂	U ₃₃	U ₁₂	U ₁₃	U ₂₃
Costibite	Co	2a	0.2806(3)	0	0	0.69(3)	0.54(3)	0.45(3)	-0.03(3)	0	0
	Sb	2a	0.0412(1)	0.3740(3)	0	0.68(2)	0.54(1)	0.45(1)	-0.05(2)	0	0
	S	2a	0.4540(5)	0.6337(5)	0	0.68(6)	0.49(6)	0.35(4)	-0.03(6)	0	0
Paracostibite	Co	8c	0.0136(2)	0.1657(2)	0.3841(1)	0.35(2)	0.41(2)	0.28(2)	0.00(2)	-0.03(2)	0.01(2)
	Sb	8c	0.1180(1)	0.0500(1)	0.1800(1)	0.39(1)	0.40(1)	0.32(1)	-0.02(1)	0.03(1)	-0.02(1)
	S	8c	-0.1333(3)	0.3095(3)	0.0659(2)	0.45(4)	0.48(4)	0.23(4)	-0.07(4)	0.01(4)	0.01(3)

*The anisotropic temperature factors are expressed in the form $T = \exp[-2\pi^2(U_1x^2 + 2U_2xy + U_3y^2 + \dots)]$.

661, 273, 164, 505, 084, and 006. For paracostibite 52 reflections, with 2θ between 53° and 58° , consisting of the equivalents of 2.1.15, 276, 467, 539, 638, 3.4.11, 0.0.16 and 800 were used. The refined unit-cell dimensions are given in Table 1, with $\alpha = \beta = \gamma = 90.00(1)^\circ$ for each material.

The intensity data were collected using graphite-monochromated MoK α radiation. The $\theta/2\theta$ scan width, 2.4 to 3.5° for costibite and 2.0 to 3.1° for paracostibite, was adjusted automatically for $\alpha_1 - \alpha_2$ dispersion. The background counts were measured on each side of the peak for 45 seconds, and the 2θ scan rate was 2° per minute. The intensities of three reference reflections were recorded after every 50 measurements in order to monitor the crystal alignment and instrument stability. No significant variations were noted during data collection.

The initial data collection for both materials was done with a 2θ limit of 60° (Gabe *et al.* 1970). The occurrence of negative temperature factors in the subsequent refinement was attributed to both insufficient intensity data and lack of absorption corrections, and data collection was repeated for both materials with a 2θ limit of 120° .

For costibite the hkl segment was collected twice and the hkl segment once, and for paracostibite the hkl segment was collected once. These data yielded 894 reflections of which 843 were considered to have net intensities above the 10% significance level [*i.e.*, $I_{net} > 1.65\sigma(I)$] for costibite, and 3085 reflections with 1886 significant for paracostibite. These intensities were adjusted for absorption effects using a generalized Gaussian procedure (Gabe & O'Byrne 1970).

STRUCTURE SOLUTION AND REFINEMENT

All calculations in these investigations were done on a CDC 6400 computer with the X-RAY system of crystallographic programs (Stewart *et al.* 1972). Lorentz and polarization factors were applied to the intensity data, and structure factors were calculated for both materials using the scattering factors of Doyle & Turner (1968) for neutral atoms. The structures were solved

using Patterson and heavy atom techniques. The atomic sites were readily established in each case, and their identification as cobalt, antimony or sulphur was made from electron-density considerations. The atoms occupy the special positions 2a ($x, y, 0$) of $Pn2_1m$ for costibite, and the general positions 8c (x, y, z) of $Pbca$ for paracostibite.

Refinement was done by difference-Fourier and full-matrix least-squares methods. During refinement, the y parameter of the cobalt atom

TABLE 3. DISTANCES AND ANGLES

	Costibite		Paracostibite	
<i>Cobalt Octahedron</i>				
Distances:	Co-Sb	2.480(2)	Co-Sb	2.551(1)
	Co-Sb(a)	2.502(2)	Co-Sb(1)	2.521(1)
	Co-Sb(b)	2.502(2)	Co-Sb(2)	2.525(1)
	Co-S(c)	2.303(3)	Co-S(3)	2.291(2)
	Co-S(d)	2.354(2)	Co-S(4)	2.306(2)
	Co-S(e)	2.354(2)	Co-S(5)	2.306(2)
Angles:	Sb-Co-Sb(a)	87.99(5)	Sb-Co-Sb(1)	82.48(3)
	Sb-Co-Sb(b)	87.99(5)	Sb-Co-Sb(2)	92.36(3)
	Sb(a)-Co-Sb(b)	92.32(6)	Sb(1)-Co-Sb(2)	83.18(3)
	S(c)-Co-S(d)	96.18(8)	S(3)-Co-S(4)	86.47(6)
	S(c)-Co-S(e)	96.18(8)	S(3)-Co-S(5)	94.36(6)
	S(d)-Co-S(e)	100.10(8)	S(4)-Co-S(5)	90.35(6)
	Sb(b)-Co-S(c)	83.65(6)	Sb(2)-Co-S(3)	90.61(5)
	Sb(a)-Co-S(d)	83.65(6)	Sb(1)-Co-S(4)	95.82(5)
	Sb(a)-Co-S(e)	87.48(5)	Sb(1)-Co-S(5)	87.08(5)
	Sb(b)-Co-S(e)	87.48(5)	Sb(2)-Co-S(5)	95.91(5)
	Sb-Co-S(4)	88.01(7)	Sb-Co-S(4)	85.18(5)
	Sb-Co-S(5)	88.01(7)	Sb-Co-S(5)	97.04(5)
	Sb-Co-S(3)	173.45(8)	Sb-Co-S(3)	165.89(5)
	Sb(a)-Co-S(e)	174.42(7)	Sb(1)-Co-S(5)	173.74(5)
	Sb(b)-Co-S(d)	174.42(7)	Sb(2)-Co-S(4)	177.45(5)
<i>Antimony Tetrahedron</i>				
Distances:	Sb-Co	2.480(2)	Sb-Co	2.551(1)
	Sb-Co(f)	2.502(2)	Sb-Co(4)	2.525(1)
	Sb-Co(g)	2.502(2)	Sb-Co(5)	2.521(1)
	Sb-S	2.521(3)	Sb-S	2.510(2)
Angles:	Co(f)-Sb-Co(g)	92.32(5)	Co(4)-Sb-Co(5)	115.98(3)
	Co-Sb-Co(f)	123.71(4)	Co-Sb-Co(4)	116.57(3)
	Co-Sb-Co(g)	123.71(4)	Co-Sb-Co(5)	114.91(3)
	Co-Sb-S	98.98(7)	Co-Sb-S	100.89(5)
	Co(f)-Sb-S	108.93(6)	Co(4)-Sb-S	102.86(5)
	Co(g)-Sb-S	108.93(6)	Co(5)-Sb-S	102.13(5)
<i>Sulphur Tetrahedron</i>				
Distances:	S-Co(h)	2.303(3)	S-Co(6)	2.290(2)
	S-Co(i)	2.354(2)	S-Co(7)	2.306(2)
	S-Co(j)	2.354(2)	S-Co(8)	2.306(2)
	S-Sb	2.521(3)	S-Sb	2.510(2)
Angles:	Co(i)-S-Co(j)	100.10(7)	Co(7)-S-Co(8)	123.18(7)
	Co(h)-S-Co(i)	120.71(10)	Co(6)-S-Co(7)	126.32(7)
	Co(h)-S-Co(j)	120.71(10)	Co(6)-S-Co(8)	93.53(6)
	Co(h)-S-Sb	105.53(10)	Co(6)-S-Sb	108.15(7)
	Co(i)-S-Sb	103.78(8)	Co(7)-S-Sb	99.20(6)
	Co(j)-S-Sb	103.78(8)	Co(8)-S-Sb	104.71(6)

Distances and angles are listed to show comparative values for costibite and paracostibite with atoms in similar orientation.

Co, Sb and S are at x, y, z . Sites of equivalent atoms are as listed below.

Costibite		Paracostibite	
(a)	$-x, -y+z, -z-z$	(1)	$-x+z, y, z-z$
(b)	$-x, -y+z, z-z$	(2)	$-x, y+z, z-z$
(c)	$x, -1+y, z$	(3)	$x, y, z+z$
(d)	$1-x, -y+z, -z-z$	(4)	$-x, -y+z, z-z$
(e)	$1-x, -y+z, z-z$	(5)	$x+z, y, z-z$
(f)	$-x, y+z, z-z$	(6)	$x, y-z, -z+z$
(g)	$-x, y+z, -z-z$		
(h)	$x, 1+y, z$		
(i)	$1-x, y+z, z-z$		
(j)	$1-x, y+z, -z-z$		

in costibite was fixed because of the polar space group. Anomalous dispersion corrections (Cromer & Liberman 1970) were introduced for both structures, and in the case of costibite which

is non-centric, the absolute configuration was established by least-squares refinement of both enantiomorphs. The final atomic and thermal parameters are listed in Table 2, and the calculated bond lengths and angles are listed in Table 3. The final R values ($\Sigma|\Delta F|/\Sigma|F_o|$) are 0.046 and 0.053, "less thans" omitted, for costibite and paracostibite, respectively. The observed and calculated structure factors are listed in Tables 6 and 7.

TABLE 4

Costibite ($Pn2_1m$)				This study				Rammelsbergite ($Pn2_1m$)†			
$a=4.873, b=5.852, c=3.608\text{\AA}$								$a=4.88, b=5.90, c=3.60\text{\AA}$			
	x	y	z		x	y	z		x	y	z
Co	$2a$	0.28	0	0	Ni	$2a$	$\frac{1}{2}$	$\frac{1}{2}$	$\frac{1}{2}$	$\frac{1}{2}$	$\frac{1}{2}$
		0.72	$\frac{1}{2}$	$\frac{1}{2}$			0	0			0
Sb	$2a$	0.04	0.37	0	As	$4g$	0.28	0.87	0.22	0.37	0
		0.96	0.87	$\frac{1}{2}$			0.72	0.13			$\frac{1}{2}$
S	$2a$	0.45	0.63	0			0.78	0.63			0
		0.55	0.13	$\frac{1}{2}$							

†Kaiman (1947). Rammelsbergite data reoriented to conventional marcasite setting, kX units converted to \AA .

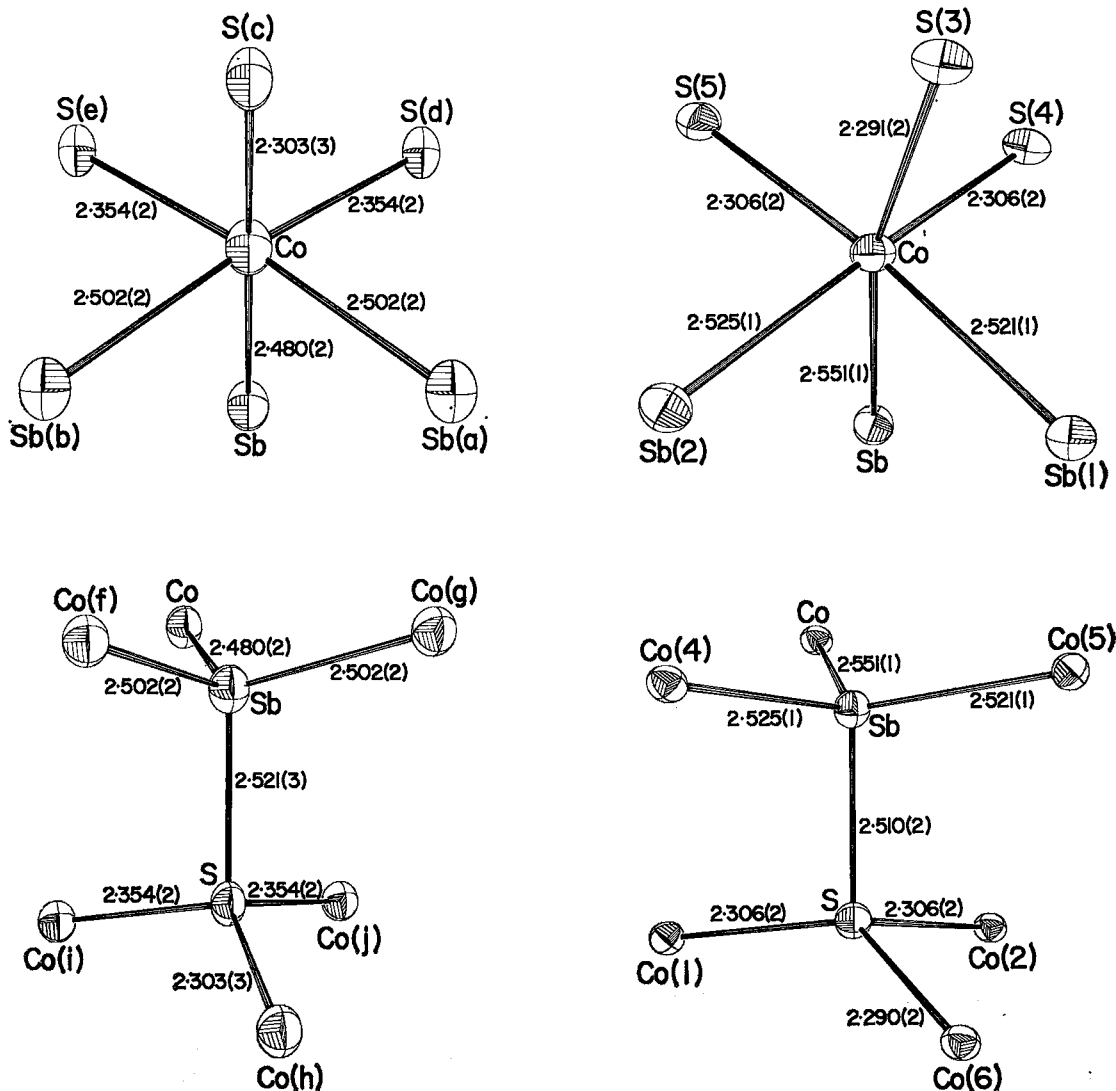


FIG. 1. The coordination of each atom type in costibite (left), and paracostibite (right), showing the interatomic distances (in \AA). The estimated standard deviations are given in parentheses. The atoms are shown as thermal ellipsoids, plotted at the 99% probability limit (Johnson 1965).

(β -NiAs₂) reported by Kaiman (1947). The sites occupied by antimony and sulphur in costibite are equivalent to the sites occupied by arsenic in rammelsbergite. One of the glide planes of the rammelsbergite space group, *Pnmm* (No. 58), is absent in costibite and this results in the space group *Pn2₁m* (No. 31).

The non-standard setting of this space group, which was chosen during interpretation of the Patterson map, facilitates the comparison of these structures. As shown in Table 4, an origin shift of $\frac{1}{4}$, $\frac{1}{2}$, $\frac{1}{2}$ results in costibite parameters that compare closely with those for rammelsbergite.

Similarly, the structure of paracostibite (CoSbS) is directly comparable to that of paramrammelsbergite (α -NiAs₂) reported by Stassen & Heyding (1968). The space group is *Pbca* for both structures, and the atomic parameters reported for paramrammelsbergite can be compared directly with those for paracostibite by an origin shift of $z = \frac{1}{2}$, as shown in Table 5.

The coordination around each atom type is similar in the two structures. Cobalt is octahedrally-coordinated to three antimony plus three sulphur (Fig. 1a, b), and sulphur and antimony are tetrahedrally coordinated to three cobalt plus one antimony and three cobalt plus one sulphur, respectively (Fig. 1c, d). The tetrahedra are interpenetrating with the Sb-S bond shared, and with angles ranging between 92° and 126° . It should be noted that the angular distortion of the Sb tetrahedron in costibite agrees more closely with that of the S rather than the Sb tetrahedron in paracostibite, and vice versa. As expected, the Co-Sb bonds are longer than the Co-S bonds. In cobaltite (CoAsS), which has the pyrite-type structure, Co-S bonds of 2.26, 2.29 and 2.36\AA were reported by Giese & Kerr (1965). Wyckoff (1960) includes Co-S and Co-Sb bonds of 2.33 and 2.58\AA , respectively, for CoS and CoSb, both of which have the hexagonal NiAs-type structure.

Costibite has the marcasite-type structure composed of staggered layers of Co octahedra, with the Sb and S atoms occupying layers at $x \approx 0$ and $x \approx \frac{1}{2}$, respectively, as shown in Figure 2. Each octahedron shares an edge with two other octahedra in the same layer, and the six corners are shared with corners of four octahedra above and four below the layer.

The paracostibite structure consists of layers of atoms perpendicular to the *c*-axis, with the

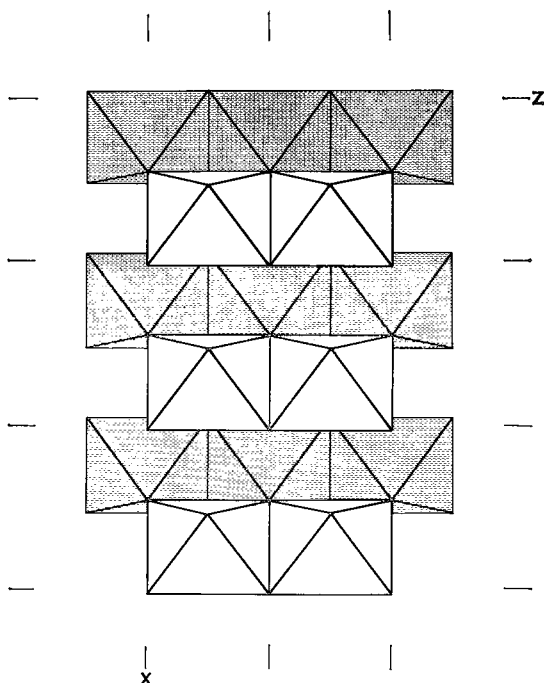


FIG. 2. The costibite structure in terms of the Co octahedra. The edges of the octahedra are joins between Sb and S atoms.

face-centered Co layers alternately stacked as pyrite-type (100) planes and marcasite-type (101) planes. In the paracostibite structure, these alternating layers have every second marcasite-type layer in reverse orientation. This arrangement has been described for the structure of paramrammelsbergite by Stassen & Heyding (1968). They reported that the metal atoms of the pyrite-type and marcasite-type layers are separated by 2.63 and 3.08\AA , respectively. In paracostibite, the corresponding values for the separation of Co layers are 3.16 and 2.72\AA , respectively. With the pyrite-type layers containing Sb atoms and the marcasite-type layers containing S atoms, the reversal of separation distances is consistent with the larger ionic radius of the Sb atom.

The paracostibite structure can also be described in terms of a marcasite-type structure alone. The relationship of the costibite and paracostibite structures can be seen in Figure 3. Figure 3 (a) shows alternate segments of costibite oriented with the (101) and $(\bar{1}01)$ planes parallel to the (001) plane of paracostibite. The similarity of this arrangement to the actual structure of paracostibite, shown in Figure 3(b), is apparent. Small shifts will permit the S and Sb atoms at $y \approx \frac{3}{8}$ and $y \approx \frac{5}{8}$ in the costibite segments to coalesce, and a rearrangement of

TABLE 5

Paracostibite (<i>Pbca</i>)				Paramrammelsbergite (<i>Pbca</i>)						
This study				Stassen & Heyding (1968)						
$a=5.842, b=5.951, c=11.666\text{\AA}$				$a=5.77, b=5.84, c=11.42\text{\AA}$						
		x	y			x	y			
Co	8c	0.01	0.17	0.38	Ni	8c	$(-x, -y, -z)$	-0.02	0.18	0.87
Sb	8c	0.12	0.05	0.18	As II	8c	$(x, \frac{1}{2}-y, \frac{1}{2}+z)$	0.12	0.05	0.68
S	8c	-0.13	0.31	0.07	As I	8c	$(x, \frac{1}{2}-y, \frac{1}{2}+z)$	-0.14	0.31	0.57

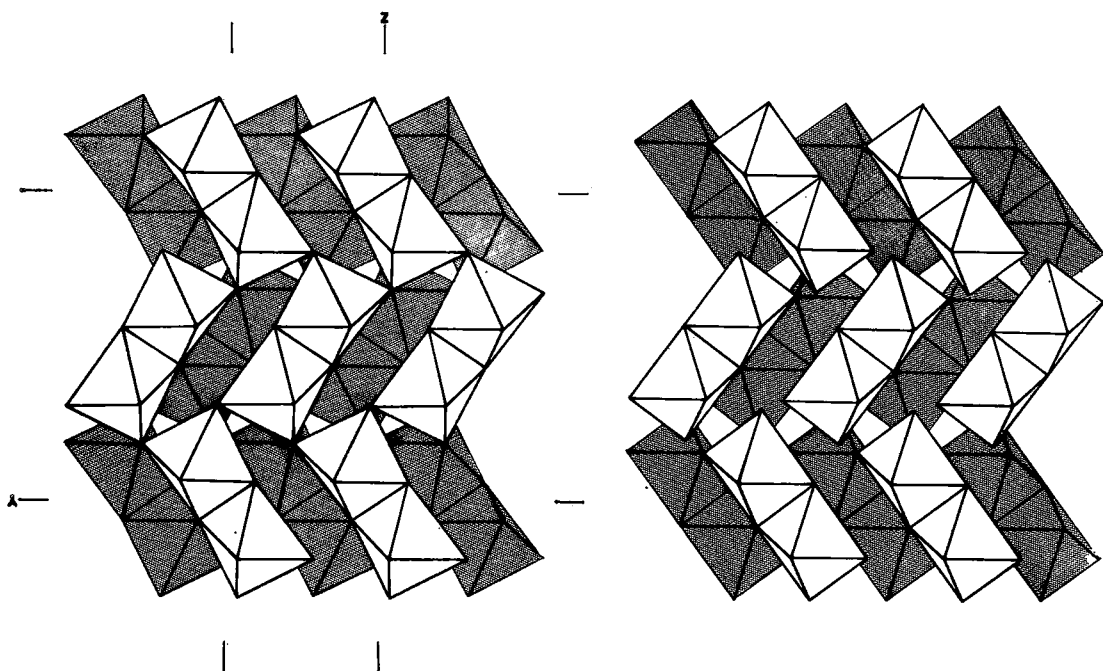


FIG. 3. The relationship of the costibite and paracostibite structures in terms of the Co octahedra. Left side shows a structural model constructed from alternate segments of costibite oriented with the (101) and $(\bar{1}01)$ planes parallel. Right side shows the paracostibite structure.

sulphur and antimony will give the paracostibite distribution. In paracostibite, each Co octahedron has one shared edge, and all corners are shared with two other octahedra.

We are indebted to Dr. L. J. Cabri for providing the natural costibite and the synthetic paracostibite used in this investigation, to Mr. J. M. Stewart for his assistance in the preliminary x-ray diffraction work, to Mr. D. Lister for the preparation of the diagrams, and to participants of the Mineral Research Program for their valuable discussions.

REFERENCES

- BUSING, W. R. (1970): *Crystallographic Computing*. F. R. Ahmed (ed.), 319-330. Copenhagen: Munksgaard.
- CABRI, L. J., HARRIS, D. C. & STEWART, J. M. (1970a): Costibite (CoSbS), a new mineral from Broken Hill, N.S.W., Australia. *Amer. Mineral.* **55**, 10-17.
- & ————— (1970b): Paracostibite (CoSbS) and nisbite (NiSb₂), new minerals from the Red Lake area, Ontario, Canada. *Can. Mineral.* **10**, 232-246.
- & ROWLAND, J. F. (1970): Willyamite redefined. *Aust. Inst. Min. Met. Proc. No. 233*, 95-100.
- CROMER, D. T. & LIBERMAN, D. (1970): Relativistic calculation of anomalous scattering factors for x-rays. *J. Chem. Phys.*, **53**, 1891-1898.
- DOYLE, P. A. & TURNER, P. S. (1968): Relativistic Hartree-Fock x-ray and electron scattering factors. *Acta Cryst.* **A24**, 390-397.
- GABE, E. J. & O'BYRNE, T. (1970): An absorption correction program for the PDP-8. A.C.A. Summer Mtg. Abstracts, paper A4.
- , ROWLAND, J. F. & HALL, S. R. (1970): The crystal structures of two forms of CoSbS. Paper presented at A.C.A. Winter Mtg. New Orleans, March 2-5, 1970.
- GIESE, R. F., JR. & KERR, P. F. (1965): The crystal structures of ordered and disordered cobaltite. *Amer. Mineral.* **50**, 1002-1014.
- JOHNSON, C. K. (1965): ORTEP: A fortran thermal-ellipsoid plot program for crystal structure illustrations. *U.S. Clearinghouse Red. Sci. Tech. Info. Rept.* ORNL-3794.
- KAIMAN, S. (1947): The crystal structure of rammelsbergite, NiAs₂. *Univ. Toronto Studies, Geol. Ser.* **51**, 49-58.
- STASSEN, W. N. & HEYDING, R. D. (1968): Crystal structures of RuSe₂, OsSe₂, PtAs₂ and α -NiAs₂. *Can. J. Chem.* **46**, 2159-2163.
- STEWART, J. M., KRUGER, G. L., AMMON, H. L., DICKINSON, C. & HALL, S. R. (1972): The x-ray system of crystallographic programs. *U. Maryland Tech. Rept.* TR-192.
- WYCKOFF, R. W. G. (1960): *Crystal Structures*, **1**, (1st edit. with supplements). Interscience, New York.

Manuscript received February 1975.

TABLE 7. pt. 1. OBSERVED AND CALCULATED STRUCTURE FACTORS FOR PARACOSTIBITE*

Table with multiple columns of numerical data, organized into groups by Miller indices (e.g., 00L, 01L, 02L, 03L, 04L, 05L, 06L, 07L, 08L, 09L, 10L, 11L, 12L, 13L, 14L, 15L, 16L, 17L, 18L, 19L, 20L, 21L, 22L, 23L, 24L, 25L, 26L, 27L, 28L, 29L, 30L, 31L, 32L, 33L, 34L, 35L, 36L, 37L, 38L, 39L, 40L, 41L, 42L, 43L, 44L, 45L, 46L, 47L, 48L, 49L, 50L, 51L, 52L, 53L, 54L, 55L, 56L, 57L, 58L, 59L, 60L, 61L, 62L, 63L, 64L, 65L, 66L, 67L, 68L, 69L, 70L, 71L, 72L, 73L, 74L, 75L, 76L, 77L, 78L, 79L, 80L, 81L, 82L, 83L, 84L, 85L, 86L, 87L, 88L, 89L, 90L, 91L, 92L, 93L, 94L, 95L, 96L, 97L, 98L, 99L, 100L, 101L, 102L, 103L, 104L, 105L, 106L, 107L, 108L, 109L, 110L, 111L, 112L, 113L, 114L, 115L, 116L, 117L, 118L, 119L, 120L, 121L, 122L, 123L, 124L, 125L, 126L, 127L, 128L, 129L, 130L, 131L, 132L, 133L, 134L, 135L, 136L, 137L, 138L, 139L, 140L, 141L, 142L, 143L, 144L, 145L, 146L, 147L, 148L, 149L, 150L, 151L, 152L, 153L, 154L, 155L, 156L, 157L, 158L, 159L, 160L, 161L, 162L, 163L, 164L, 165L, 166L, 167L, 168L, 169L, 170L, 171L, 172L, 173L, 174L, 175L, 176L, 177L, 178L, 179L, 180L, 181L, 182L, 183L, 184L, 185L, 186L, 187L, 188L, 189L, 190L, 191L, 192L, 193L, 194L, 195L, 196L, 197L, 198L, 199L, 200L, 201L, 202L, 203L, 204L, 205L, 206L, 207L, 208L, 209L, 210L, 211L, 212L, 213L, 214L, 215L, 216L, 217L, 218L, 219L, 220L, 221L, 222L, 223L, 224L, 225L, 226L, 227L, 228L, 229L, 230L, 231L, 232L, 233L, 234L, 235L, 236L, 237L, 238L, 239L, 240L, 241L, 242L, 243L, 244L, 245L, 246L, 247L, 248L, 249L, 250L, 251L, 252L, 253L, 254L, 255L, 256L, 257L, 258L, 259L, 260L, 261L, 262L, 263L, 264L, 265L, 266L, 267L, 268L, 269L, 270L, 271L, 272L, 273L, 274L, 275L, 276L, 277L, 278L, 279L, 280L, 281L, 282L, 283L, 284L, 285L, 286L, 287L, 288L, 289L, 290L, 291L, 292L, 293L, 294L, 295L, 296L, 297L, 298L, 299L, 300L, 301L, 302L, 303L, 304L, 305L, 306L, 307L, 308L, 309L, 310L, 311L, 312L, 313L, 314L, 315L, 316L, 317L, 318L, 319L, 320L, 321L, 322L, 323L, 324L, 325L, 326L, 327L, 328L, 329L, 330L, 331L, 332L, 333L, 334L, 335L, 336L, 337L, 338L, 339L, 340L, 341L, 342L, 343L, 344L, 345L, 346L, 347L, 348L, 349L, 350L, 351L, 352L, 353L, 354L, 355L, 356L, 357L, 358L, 359L, 360L, 361L, 362L, 363L, 364L, 365L, 366L, 367L, 368L, 369L, 370L, 371L, 372L, 373L, 374L, 375L, 376L, 377L, 378L, 379L, 380L, 381L, 382L, 383L, 384L, 385L, 386L, 387L, 388L, 389L, 390L, 391L, 392L, 393L, 394L, 395L, 396L, 397L, 398L, 399L, 400L, 401L, 402L, 403L, 404L, 405L, 406L, 407L, 408L, 409L, 410L, 411L, 412L, 413L, 414L, 415L, 416L, 417L, 418L, 419L, 420L, 421L, 422L, 423L, 424L, 425L, 426L, 427L, 428L, 429L, 430L, 431L, 432L, 433L, 434L, 435L, 436L, 437L, 438L, 439L, 440L, 441L, 442L, 443L, 444L, 445L, 446L, 447L, 448L, 449L, 450L, 451L, 452L, 453L, 454L, 455L, 456L, 457L, 458L, 459L, 460L, 461L, 462L, 463L, 464L, 465L, 466L, 467L, 468L, 469L, 470L, 471L, 472L, 473L, 474L, 475L, 476L, 477L, 478L, 479L, 480L, 481L, 482L, 483L, 484L, 485L, 486L, 487L, 488L, 489L, 490L, 491L, 492L, 493L, 494L, 495L, 496L, 497L, 498L, 499L, 500L, 501L, 502L, 503L, 504L, 505L, 506L, 507L, 508L, 509L, 510L, 511L, 512L, 513L, 514L, 515L, 516L, 517L, 518L, 519L, 520L, 521L, 522L, 523L, 524L, 525L, 526L, 527L, 528L, 529L, 530L, 531L, 532L, 533L, 534L, 535L, 536L, 537L, 538L, 539L, 540L, 541L, 542L, 543L, 544L, 545L, 546L, 547L, 548L, 549L, 550L, 551L, 552L, 553L, 554L, 555L, 556L, 557L, 558L, 559L, 560L, 561L, 562L, 563L, 564L, 565L, 566L, 567L, 568L, 569L, 570L, 571L, 572L, 573L, 574L, 575L, 576L, 577L, 578L, 579L, 580L, 581L, 582L, 583L, 584L, 585L, 586L, 587L, 588L, 589L, 590L, 591L, 592L, 593L, 594L, 595L, 596L, 597L, 598L, 599L, 600L, 601L, 602L, 603L, 604L, 605L, 606L, 607L, 608L, 609L, 610L, 611L, 612L, 613L, 614L, 615L, 616L, 617L, 618L, 619L, 620L, 621L, 622L, 623L, 624L, 625L, 626L, 627L, 628L, 629L, 630L, 631L, 632L, 633L, 634L, 635L, 636L, 637L, 638L, 639L, 640L, 641L, 642L, 643L, 644L, 645L, 646L, 647L, 648L, 649L, 650L, 651L, 652L, 653L, 654L, 655L, 656L, 657L, 658L, 659L, 660L, 661L, 662L, 663L, 664L, 665L, 666L, 667L, 668L, 669L, 670L, 671L, 672L, 673L, 674L, 675L, 676L, 677L, 678L, 679L, 680L, 681L, 682L, 683L, 684L, 685L, 686L, 687L, 688L, 689L, 690L, 691L, 692L, 693L, 694L, 695L, 696L, 697L, 698L, 699L, 700L, 701L, 702L, 703L, 704L, 705L, 706L, 707L, 708L, 709L, 710L, 711L, 712L, 713L, 714L, 715L, 716L, 717L, 718L, 719L, 720L, 721L, 722L, 723L, 724L, 725L, 726L, 727L, 728L, 729L, 730L, 731L, 732L, 733L, 734L, 735L, 736L, 737L, 738L, 739L, 740L, 741L, 742L, 743L, 744L, 745L, 746L, 747L, 748L, 749L, 750L, 751L, 752L, 753L, 754L, 755L, 756L, 757L, 758L, 759L, 760L, 761L, 762L, 763L, 764L, 765L, 766L, 767L, 768L, 769L, 770L, 771L, 772L, 773L, 774L, 775L, 776L, 777L, 778L, 779L, 780L, 781L, 782L, 783L, 784L, 785L, 786L, 787L, 788L, 789L, 790L, 791L, 792L, 793L, 794L, 795L, 796L, 797L, 798L, 799L, 800L, 801L, 802L, 803L, 804L, 805L, 806L, 807L, 808L, 809L, 810L, 811L, 812L, 813L, 814L, 815L, 816L, 817L, 818L, 819L, 820L, 821L, 822L, 823L, 824L, 825L, 826L, 827L, 828L, 829L, 830L, 831L, 832L, 833L, 834L, 835L, 836L, 837L, 838L, 839L, 840L, 841L, 842L, 843L, 844L, 845L, 846L, 847L, 848L, 849L, 850L, 851L, 852L, 853L, 854L, 855L, 856L, 857L, 858L, 859L, 860L, 861L, 862L, 863L, 864L, 865L, 866L, 867L, 868L, 869L, 870L, 871L, 872L, 873L, 874L, 875L, 876L, 877L, 878L, 879L, 880L, 881L, 882L, 883L, 884L, 885L, 886L, 887L, 888L, 889L, 890L, 891L, 892L, 893L, 894L, 895L, 896L, 897L, 898L, 899L, 900L, 901L, 902L, 903L, 904L, 905L, 906L, 907L, 908L, 909L, 910L, 911L, 912L, 913L, 914L, 915L, 916L, 917L, 918L, 919L, 920L, 921L, 922L, 923L, 924L, 925L, 926L, 927L, 928L, 929L, 930L, 931L, 932L, 933L, 934L, 935L, 936L, 937L, 938L, 939L, 940L, 941L, 942L, 943L, 944L, 945L, 946L, 947L, 948L, 949L, 950L, 951L, 952L, 953L, 954L, 955L, 956L, 957L, 958L, 959L, 960L, 961L, 962L, 963L, 964L, 965L, 966L, 967L, 968L, 969L, 970L, 971L, 972L, 973L, 974L, 975L, 976L, 977L, 978L, 979L, 980L, 981L, 982L, 983L, 984L, 985L, 986L, 987L, 988L, 989L, 990L, 991L, 992L, 993L, 994L, 995L, 996L, 997L, 998L, 999L, 1000L.

TABLE 7. pt. 2. OBSERVED AND CALCULATED STRUCTURE FACTORS FOR PARA-COSTIBITE.

Table with multiple columns of numerical data representing observed and calculated structure factors for Paracostibite. The table is organized into several vertical sections, each containing a list of hkl indices and their corresponding observed (O) and calculated (C) values. The data is presented in a grid-like format with varying column widths and row alignments.

TABLE 7. pt. 3. OBSERVED AND CALCULATED STRUCTURE FACTORS FOR PARACOSTIBITE*

Table with multiple columns containing numerical data for structure factors. The table is organized into several vertical sections, each with a header indicating the type of structure factor (e.g., 7.0L, 7.1L, 8.0L, 8.1L, 9.0L, 9.1L, 10.0L, 10.1L, 11.0L, 11.1L, 12.0L, 12.1L, 13.0L, 13.1L, 14.0L, 14.1L, 15.0L, 15.1L, 16.0L, 16.1L, 17.0L, 17.1L, 18.0L, 18.1L, 19.0L, 19.1L, 20.0L, 20.1L, 21.0L, 21.1L, 22.0L, 22.1L). Each section contains a list of numbers representing observed and calculated values for various reflections.

*The structure factors are listed in blocks of constant h/k in columns of I, [F_o] × 10, and [F_c] × 10.